

## Boromuscovite, a new member of the mica group, from the Little Three mine pegmatite, Ramona district, San Diego County, California

EUGENE E. FOORD

U.S. Geological Survey, M.S. 905, Box 25046 Denver Federal Center, Denver, Colorado 80225, U.S.A.

ROBERT F. MARTIN

Department of Geological Sciences, McGill University, 3450 University Street, Montreal, Quebec H3A 2A7, Canada

JOAN J. FITZPATRICK

U.S. Geological Survey, M.S. 939, Box 25046 Denver Federal Center, Denver, Colorado 80225, U.S.A.

JOSEPH E. TAGGART, JR., JAMES G. CROCK

U.S. Geological Survey, M.S. 973, Box 25046 Denver Federal Center, Denver, Colorado 80225, U.S.A.

### ABSTRACT

Boromuscovite, ideally  $\text{KAl}_2(\text{Si}_3\text{B})\text{O}_{10}(\text{OH},\text{F})_2$ , in which  $^{141}\text{Al}$  is replaced by B relative to muscovite, occurs as a late-stage, postpocket rupture mineral within the New Spaulding Pocket, main Little Three pegmatite dike, Ramona district, San Diego County, California. The mineral is white to cream colored and occurs as a porcelaneous veneer and coating on primary minerals. The average grain size is less than 3–4  $\mu\text{m}$ , but the coatings may be as much as 1 cm or more thick. Fragments of topaz, albite, elbaite, and other pocket minerals are included in the coating. The boromuscovite precipitated from a late-stage hydrothermal fluid; it occurs only as a snowlike coating.

Chemical analysis yielded (wt%):  $\text{SiO}_2$  48.1,  $\text{Al}_2\text{O}_3$  28.1,  $\text{B}_2\text{O}_3$  7.0,  $\text{CaO}$  0.1,  $\text{MgO}$  0.15,  $\text{Fe}_2\text{O}_3$  0.1,  $\text{MnO}$  0.08,  $\text{P}_2\text{O}_5$  <0.05,  $\text{TiO}_2$  <0.01,  $\text{K}_2\text{O}$  11.0,  $\text{Na}_2\text{O}$  <0.05,  $\text{Li}_2\text{O}$  0.05,  $\text{Rb}_2\text{O}$  0.52,  $\text{Cs}_2\text{O}$  0.05, F 0.76,  $\text{H}_2\text{O}^+$  4.55,  $\text{H}_2\text{O}^-$  0.22, O = F 0.32, total 100.46. An empirical formula calculated on the basis of 12 O + OH + F is:  $(\text{K}_{0.89}\text{Rb}_{0.02}\text{Ca}_{0.01})_{20.92}(\text{Al}_{1.93}\text{Li}_{0.01}\text{Mg}_{0.01})_{21.95}(\text{Si}_{3.06}\text{B}_{0.77}\text{Al}_{0.17})_{24.00}\text{O}_{9.82}[(\text{OH})_{2.02}\text{F}_{0.16}]_{22.18}$ . The mineral is a mixture of about equal amounts of  $2M_1$  and  $1M$  polytypes. Refined unit-cell parameters for both polytypes are significantly smaller than those for muscovite:  $2M_1$ ,  $a = 5.075(1)$ ,  $b = 8.794(4)$ ,  $c = 19.815(25)$  Å,  $\beta = 95.59(3)^\circ$ ;  $1M$ ,  $a = 5.077(1)$ ,  $b = 8.775(3)$ ,  $c = 10.061(2)$  Å,  $\beta = 101.31(2)^\circ$ .  $D_{\text{calc}}$  for the  $2M_1$  and  $1M$  polytypes are 2.89 g/cm<sup>3</sup> and 2.90 g/cm<sup>3</sup>, respectively.  $D_{\text{obs}}$  of the mixture is 2.81 g/cm<sup>3</sup>.

In aggregate, the mineral has a Mohs hardness of 2.5–3, white streak, a dull to porcelaneous luster, perfect {001} cleavage, a poor parting on {010}, poor to subconchoidal fracture, and no fluorescence or luminescence. Optical properties are (for Na light): biaxial (–),  $\alpha = 1.557$ ,  $\beta = 1.587$ ,  $\gamma = 1.593$  (all  $\pm 0.002$ ),  $2V_{x\text{ meas}} = 44(2)^\circ$ ,  $2V_{x\text{ calc}} = 47.5^\circ$ , dispersion is  $r > v$  weak. For the  $2M_1$  polytype, the OAP is normal to (010),  $X:c = -1^\circ$ ,  $Y:a = +2^\circ$ ,  $Z = b$ ;  $X$  is in the acute angle of  $\beta$  and  $Y$  is in the obtuse angle of  $\beta$ . The mineral shows no absorption or pleochroism.

Boromuscovite crystallized from the evolved fluid phase present after the growth of the primary minerals in the New Spaulding Pocket. The coexistence of the  $2M_1$  and  $1M$  polytypes is consistent with growth in the interval 350–400 °C, a range consistent with fluid-inclusion geothermometry on pocket minerals in related pegmatitic occurrences.

### INTRODUCTION

The Little Three layered pegmatite-aplite intrusion is located in the Ramona pegmatite district of central San Diego County, California (Foord et al., 1989). Bodies of granitic pegmatite on the Little Three mine property have been the subject of study since their discovery in 1903. The voluminous literature has been summarized in Foord et al. (1989). In June, 1976, while working the Little Three main dike for gem- and specimen-quality tourmaline and

topaz, the mine owner, Louis B. Spaulding, Jr., uncovered a zone of pocket mineralization. The New Spaulding Pocket (NSP) was the largest and most productive of the pockets in this zone (see Stern et al., 1986). The NSP, with a volume of approximately 2.2 m<sup>3</sup>, occupied an irregularly shaped cavity averaging 0.25 m in height.

The contents of the NSP included quartz, tourmaline (schorl-elbaite), blue and colorless topaz, maximum microcline “pillars,” clear and smoky quartz, cleavelandite,



Fig. 1. SEM photograph of boromuscovite from the NSP. Scale bar equals 4  $\mu\text{m}$ .

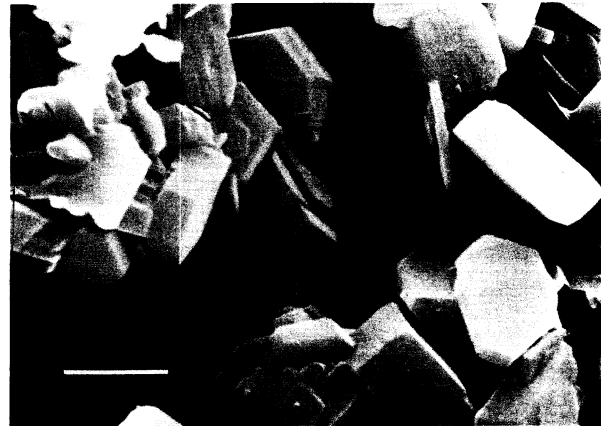


Fig. 2. SEM photograph of boromuscovite from the NAP showing euhedral pseudo-hexagonal flakes. Scale bar equals 2  $\mu\text{m}$ .

F-rich lepidolite, microlite-uranmicrolite, and a new polymorph of stibiocolumbite-stibiotantalite. Coarse-grained ( $\geq 5$  cm across) euhedral books of lepidolite-*1M* irregularly lined the floor. Tourmaline crystals were attached to the roof within a mass of coarsely bladed cleavelandite, with lesser amounts of cleavelandite ( $\sim 20\%$ ) rooted to the floor of the pocket. Several lepidolite crystals were attached to elbaite specimens on the roof (Stern et al., 1986). Large blue topaz crystals were removed from the sides of the pocket, the majority occurring on the floor. Small colorless topaz crystals grew on the elbaite faces along the roof of the pocket.

All minerals (principally lepidolite, quartz, microcline, and topaz) on the floor, including those broken off during pocket rupture and fragments of crystals lying on the floor, were coated with a fine-grained, hard, porcelainous substance, which was subsequently determined to be boromuscovite. Deposition of the boromuscovite occurred after the initial rupturing event in the NSP as well as after another period of primary mineral growth and crystal repair. At a lower temperature, circulation of an aqueous solution, laden with crystal fragments, through the pocket resulted in abrasion of the boromuscovite coating and underlying minerals. Pockets peripheral to the NSP that were not reopened to migrating solutions ("dry pockets") contained only the snowlike coating of boromuscovite, muscovite, or cookeite. Hydrothermal pocket clays, consisting chiefly of montmorillonite, were described by Foord et al. (1986).

The name boromuscovite and the status of this mineral as a new species (89-027) were approved by the IMA Commission on New Minerals and Mineral Names (CNMMN). Type material (no. 166821) was deposited at the U.S. National Museum of Natural History.

#### PHYSICAL PROPERTIES

Boromuscovite is buff to pale cream colored, has an earthy to porcelainous luster, a white streak, a hardness of 2.5–3, a poor to subconchoidal fracture (all in compact masses), one perfect cleavage  $\{001\}$ , a poor parting on

$\{010\}$ , is opaque, and does not fluoresce or luminesce (Figs. 1 and 2).  $D_{\text{meas}}$  on a Berman microbalance and by suspension in bromoform-acetone mixture is 2.81  $\text{g}/\text{cm}^3$ .  $D_{\text{calc}}$  is 2.89 and 2.90  $\text{g}/\text{cm}^3$  for the *2M*, and *1M* polytypes, respectively. The 0.09  $\text{g}/\text{cm}^3$  difference probably results from air trapped in the fine-grained masses of boromuscovite.

#### CHEMISTRY

Boromuscovite was analyzed by a variety of methods and, in some instances, in duplicate. An emission spectrographic analysis (Table 1) showed the presence of approximately 3 wt% B. Electron microprobe analyses (ARL SEMQ) indicated that the material is homogeneous on the micrometer scale, and X-ray fluorescence analysis (PW1600) yielded the same composition determined by electron microprobe. Concentrations of  $\text{H}_2\text{O}^+$ ,  $\text{H}_2\text{O}^-$ , Li,

TABLE 1. Trace and minor element contents in boromuscovite from the New Spaulding Pocket

Element	Method	
	Emission spectroscopy	ICP-AES
Ca	0.03%	0.36%
Fe	0.1%	0.13%
Mg	0.07%	0.08%
Ti	0.01%	<0.04%
Mn	0.15%	0.07%
Ba	15	30
Be	5	<9
Ga	200	120
Li	300	240
Sr	7	40
Ge	30	n.d.
Zr	15	n.d.
Tl	50	n.d.
B	3.0%	2.18%
Bi	30	<20
Pb	15	<20
V	7	<10
Na	0.3%	n.d.
Rb	0.5%	n.d.
Cs	300	n.d.

Note: n.d. = not determined. All values given in ppm except where stated otherwise.

**TABLE 2.** Chemical composition of boromuscovite from the NSP

Oxide	Wt%	Analytical method(s)	EDS (wt%)
SiO <sub>2</sub>	48.1	XRF and EMP	48.13
Al <sub>2</sub> O <sub>3</sub>	28.1	XRF and EPM	25.76
B <sub>2</sub> O <sub>3</sub>	7.0	ICP-AES	n.d.
CaO	0.1	XRF and EMP	0.10
MgO	0.15	XRF, EMP, and ICP-AES	1.12
Fe <sub>2</sub> O <sub>3</sub>	0.1	XRF, EMP, and ICP-AES	0.23
MnO	0.08	XRF and ICP-AES	n.d.
P <sub>2</sub> O <sub>5</sub>	none	XRF and ICP-AES	n.d.
TiO <sub>2</sub>	none	XRF, EMP, and ICP-AES	0.06
K <sub>2</sub> O	11.0	XRF and EMP	11.51
Na <sub>2</sub> O	none	XRF and EMP	0.80
Li <sub>2</sub> O	0.05	ICP-AES	n.d.
Rb <sub>2</sub> O	0.52	emission spectroscopy and AA	n.d.
Cs <sub>2</sub> O	0.05	emission spectroscopy and AA	n.d.
F	0.76	selective-ion electrode	n.d.
H <sub>2</sub> O <sup>+</sup>	4.55	microcoulometric moisture anal.	n.d.
H <sub>2</sub> O <sup>-</sup>	0.22	microcoulometric moisture anal.	n.d.
O for F	0.32		
Total	100.46		

Note: All Fe expressed as Fe<sub>2</sub>O<sub>3</sub>. EDS analysis is an average of 11 determinations performed on single flakes. EDS analysis total recalculated to 87.79 wt% to allow for 7.0 wt% B<sub>2</sub>O<sub>3</sub>, 0.76 wt% F, and 4.55 wt% H<sub>2</sub>O<sup>+</sup>. XRF = X-ray fluorescence, EMP = electron microprobe, AA = atomic absorption. ICP-AES = inductively coupled plasma-atomic emission spectroscopy.

Rb, Cs, and F were subsequently determined to complete the characterization. ICP-AES (inductively coupled, plasma-atomic emission spectrography) analysis (Table 1) of the bulk material confirmed the previously determined chemistry.

A composite of chemical data was used to derive the bulk composition of boromuscovite (Table 2). The structural formula of boromuscovite, calculated on the basis of 12 O + OH + F, is (K<sub>0.89</sub>Rb<sub>0.02</sub>Ca<sub>0.01</sub>)<sub>20.92</sub>(Al<sub>1.93</sub>Li<sub>0.01</sub>Mg<sub>0.01</sub>)<sub>Σ1.95</sub>(Si<sub>3.06</sub>B<sub>0.77</sub>Al<sub>0.17</sub>)<sub>Σ4.00</sub>O<sub>9.82</sub>[(OH)<sub>2.02</sub>F<sub>0.16</sub>]<sub>Σ2.18</sub>.

#### X-RAY DIFFRACTION AND UNIT-CELL DATA

Power diffraction data (Table 3) were obtained using a Guinier-Hägg camera with CuK $\alpha$  radiation. Intensities were determined separately from a diffractometer trace of a randomly oriented back-packed sample, using graphite-monochromatized CuK $\alpha$  radiation, at 40 kV and 30 mA. Refined unit-cell data were obtained using a modified version of the least-squares program of Appleman and Evans (1973). A mixture of approximately equal amounts of 2M, and 1M polytypes accounts for the data. Because of the fine grain size, single-crystal X-ray studies were not possible; thus, space groups were assigned by analogy to those of muscovite.

The metric dimensions of the unit cells of the two polytypes are significantly smaller (1.1–2.5%) than those reported for both synthetic and natural B-free 2M, and 1M muscovite (Table 3). The  $\beta$  angles also are smaller. The volumes of each are 93–94% of the volume of the equivalent polytypes of muscovite.

#### OPTICAL PROPERTIES

The optical properties of boromuscovite were determined on oil-immersion grain mounts and by spindle-

**TABLE 3.** X-ray powder diffraction and unit-cell data for boromuscovite polytypes from the NSP

<i>hkl</i>	<i>d</i> <sub>calc</sub> (Å)	<i>d</i> <sub>obs</sub> (Å)	<i>I</i> / <i>I</i> <sub>0</sub>	Polytype
002	9.860	9.862	60	2M <sub>1</sub>
001	9.865	9.862		1M
004	4.930	4.929	20	2M <sub>1</sub>
002	4.933	4.929		1M
110	4.379	4.391	80	2M <sub>1</sub>
$\bar{1}11$	4.354	4.350	<10	2M <sub>1</sub>
$\bar{1}11$	4.240	4.239	40	1M
111	4.201	4.194	<10	2M <sub>1</sub>
022	4.014	4.007	40	2M <sub>1</sub>
$\bar{1}13$	3.796	3.799	10	2M <sub>1</sub>
023	3.654	3.652	10	2M <sub>1</sub>
$\bar{1}12$	3.570	3.569	100	1M
$\bar{1}14$	3.421	3.418	10	2M <sub>1</sub>
006	3.287	3.287	40	2M <sub>1</sub>
003	3.288	3.287		1M
024	3.281	3.280	20	2M <sub>1</sub>
114	3.145	3.142	10	2M <sub>1</sub>
112	3.010	3.008	80	1M
025	2.935	2.930	<10	2M <sub>1</sub>
$\bar{1}13$	2.865	2.865	20	1M
201	2.534	2.533	30	1M
200	2.525	2.524	40	2M <sub>1</sub>
$\bar{1}31$	2.504	2.505	80	1M
200	2.489	2.489	40	1M
$\bar{1}17$	2.466	2.467	<10	2M <sub>1</sub>
113	2.427	2.427	10	1M
$\bar{2}02$	2.422	2.421	10	1M
131	2.387	2.388	20	1M
$\bar{2}04$	2.342	2.341	30	2M <sub>1</sub>
201	2.309	2.309	20	1M
$\bar{2}21, 040$	2.195, 2.194	2.195	40	1M
204	2.164	2.165	20	2M <sub>1</sub>
041	2.142	2.141	10	1M
$\bar{2}22$	2.120	2.119	10	1M
$\bar{2}06$	2.104	2.104	30	2M <sub>1</sub>
135	2.086	2.087	10	2M <sub>1</sub>
202	2.065	2.066	10	1M
221	2.043	2.043	10	1M
0010	1.972	1.972	30	2M <sub>1</sub>
005	1.973	1.972		1M
204	1.954	1.954	10	1M
113	1.912	1.910	10	1M
208	1.857	1.857	<10	2M <sub>1</sub>
$\bar{2}24$	1.785	1.786	10	1M
$\bar{3}11, \bar{1}06$	1.661	1.661	10	1M
2010	1.633	1.633	10	2M <sub>1</sub>
204, $\bar{1}52$	1.601	1.601	10	1M
$\bar{1}54$	1.589	1.590	10	2M <sub>1</sub>
313	1.588	1.588	<10	1M
$\bar{2}43$	1.555	1.555	<10	1M
0212	1.539	1.539	<10	2M <sub>1</sub>
$\bar{2}06, \bar{3}23$	1.515	1.515	<10	1M
135	1.484	1.485	<10	1M
060	1.465	1.465	40	2M <sub>1</sub>

#### Unit-cell data

Boromuscovite-2M <sub>1</sub>	Muscovite-2M <sub>1</sub> , PDF 6-263	Boromuscovite-1M	Muscovite-1M PDF 7-25
<i>a</i> = 5.075(1) Å	5.190 Å	5.077(1) Å	5.208 Å
<i>b</i> = 8.794(4) Å	9.030 Å	8.775(3) Å	8.995 Å
<i>c</i> = 19.815(25) Å	20.050 Å	10.061(2) Å	10.275 Å
$\beta$ = 95.59(3)°	95.77°	101.31(2)°	101.6°
<i>V</i> = 879.7(15) Å <sup>3</sup>	934.90 Å <sup>3</sup>	439.53(14) Å <sup>3</sup>	471.5 Å <sup>3</sup>

Note: Operating conditions: Guinier-Hägg camera, CuK $\alpha$  radiation, 12-h exposure, 40 kV, 30 mA. Si internal standard (NBS). Refinements done using computer program of Appleman and Evans (1973). Intensities are from random mounts scanned with a Philips powder diffractometer.

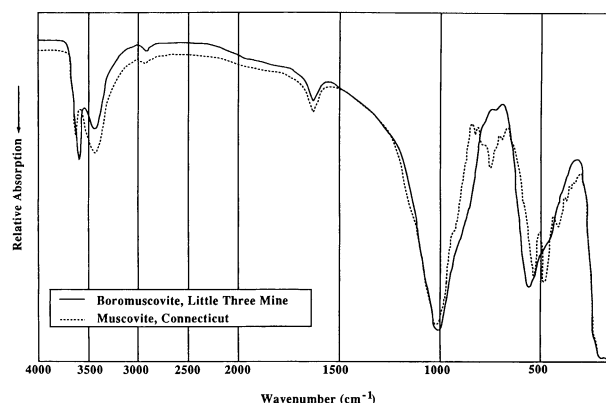


Fig. 3. IR spectra for boromuscovite and muscovite.

stage techniques, with flakes measuring about  $5\ \mu\text{m}$  across. The mineral is colorless, without pleochroism or absorption. Principal indices of refraction determined at 589 nm and  $22\ ^\circ\text{C}$  are  $\alpha = 1.557$ ,  $\beta = 1.587$ ,  $\gamma = 1.593$  (each  $\pm 0.002$ );  $2V_{x,\text{meas}} = 44(2)^\circ$  and  $2V_{x,\text{calc}} = 47.5^\circ$ . Dispersion is weak,  $r > v$ . The orientation scheme for the  $2M_1$  polytype is OAP normal to (010),  $X:c = -1^\circ$ ,  $Y:a = +2^\circ$ , and  $Z = b$ .  $X$  is in the acute angle  $\beta$ , and  $Y$  is in the obtuse angle  $\beta$ .

### TEM STUDIES

Transmission electron microscopy (TEM) studies were carried out on Philips instruments (420ST operated at 120 kV, CM30 operated at 300 kV). A 2.3-mm disk was removed from a petrographic thin section of polycrystalline boromuscovite, mounted on a Cu grid, further thinned by standard Ar ion-milling techniques, and C coated. In addition, pulverized material was sedimented on a holey-carbon substrate on a Cu grid.

Boromuscovite was found to be unstable in the electron beam and became amorphous in seconds. Selected-area diffraction patterns containing  $c^*$  were obtained from two crystals only; (001) lattice-fringe images could not be obtained before breakdown. The single row of sharp diffraction maxima along  $c^*$  confirms the 10-Å repeat. There is no evidence of a mixture of 10-Å and 20-Å, polytypes within single flakes, at least at the scale of TEM observation.

Energy-dispersive spectra were obtained on 11 grains using an EDAX Si(Li) X-ray detector and a Princeton Gamma-Tech System IV analyzer. Raw data were reduced following Livi and Veblen (1987). An average bulk composition of the mica, calculated by assuming 7.0 wt%  $\text{B}_2\text{O}_3$ , 0.76 wt% F, and 4.55 wt%  $\text{H}_2\text{O}$ , is presented in Table 2.

### INFRARED SPECTRAL STUDIES

Standard infrared absorption spectra for the region 200–4000  $\text{cm}^{-1}$  were obtained using a Perkin-Elmer 580B instrument for boromuscovite and muscovite  $2M_1$  (Fig. 3). The two spectra are similar, including the 800–1200  $\text{cm}^{-1}$  region, which contains the  $(\text{Si},\text{Al},\text{B})\text{O}_4$  stretching vibra-

tions. The OH and H-O-H bands are present at 3440  $\text{cm}^{-1}$  and 1650  $\text{cm}^{-1}$ , respectively. However, some differences also are apparent near 500  $\text{cm}^{-1}$  and 750  $\text{cm}^{-1}$ . The vibration at 750  $\text{cm}^{-1}$  may result from the substitution of tetrahedral B for Al.

### DISCUSSION

The incorporation of tetrahedrally coordinated B in phyllosilicates has been well established through studies of synthetic systems and natural examples. Noda et al. (1944) synthesized a B-rich fluorophlogopite in which tetrahedrally coordinated Al is replaced by B. Eugster and Wright (1960) synthesized Al-free, B-bearing hydrous phlogopite and biotite and probably B-bearing muscovite. Harder (1959a, 1959b) found as much as 2000 ppm B in natural micas. Manandonite,  $\text{Li}_2\text{Al}_4[(\text{Si}_2\text{AlB})\text{O}_{10}](\text{OH})_8$ , possibly a serpentine mineral, contains Al partly replaced by B (Lacroix, 1922; Hawthorne and Černý, 1982; Ranzoro et al., 1989). It is known only from Madagascar as a crust in cavities lined with elbaite, quartz, and albite. Cookeite also may contain B but in subordinate amounts (Hawthorne and Černý, 1982).

Boromuscovite is the natural analogue of a previously synthesized B-substituted mica. Boromuscovite may be a rare mica, considering the volume of chemical data available for muscovite and B-, Be-, rare-metal-, and rare-alkali-containing muscovite from granitic pegmatites.

At the time of crystallization of the pocket minerals in the NSP, the aqueous vapor phase was distinctly enriched in K, Al, B, and F. This enrichment is expressed by the abundance of F-rich lepidolite and topaz, elbaite, and potassium feldspar. In contrast, the later hydrothermal fluid, from which the boromuscovite crystallized, had become relatively depleted in F.

Boromuscovite formed from this evolved hydrothermal solution at a moderate temperature (350–400  $^\circ\text{C}$ ) and low pressure (1–2 kbar). Stagnant conditions during nucleation and growth are indicated by the snowlike character of the coating. The inferred  $P$ - $T$  conditions for the deposition of boromuscovite are based on extrapolation of temperatures of fluid-inclusion homogenization from "pocket" minerals in other pegmatite dikes in the region (Taylor et al., 1979; Foord et al., 1986). The  $P$ - $T$  conditions also are consistent with the mineral assemblages found and phase-equilibrium studies in pegmatitic systems (London, 1984, 1986a, 1986b, 1987). By analogy with findings in muscovite (Hawthorne and Černý, 1982; Frey et al., 1983; Mukhamet-Galeyev et al., 1984), the deposition of the  $2M_1$  and  $1M$  polytypes of boromuscovite presumably reflects the low temperature of its nucleation and growth (Amouric and Baronnet, 1983) rather than an arrested stage of a progressive transformation by recrystallization of the  $2M_1$  polytype, considered to be more stable at higher temperature than the  $1M$  polytype.

### ACKNOWLEDGMENTS

We thank Larry L. Jackson of the U.S. Geological Survey for the F,  $\text{H}_2\text{O}^+$ , and  $\text{H}_2\text{O}^-$  analyses. Nancy M. Conklin performed an emission

spectrographic analysis. R.M. Mahrt of the U.S. Geological Survey assisted in the collection of the IR spectra. R.F.M. thanks David R. Veblen and Kenneth J.T. Livi for their hospitality and their guidance in the use of the Philips 420ST transmission electron microscope at the Johns Hopkins University. René Veillette and Gilles L'Espérance provided access to the Philips CM30 instrument in the CM<sup>2</sup> center, Département de Génie métallurgique, Ecole Polytechnique, Montréal. R.F.M. acknowledges the support of the Natural Sciences and Engineering Research Council of Canada (grant A7721). Reviews were provided by C.G. Whitney and R.C. Erd of the U.S. Geological Survey, S.W. Bailey (University of Wisconsin) and P. Černý (University of Manitoba).

#### REFERENCES CITED

- Amouric, M., and Baronnet, A. (1983) Effect of early nucleation conditions on synthetic muscovite polytypism as seen by high-resolution transmission electron microscopy. *Physics and Chemistry of Minerals*, 9, 146–159.
- Appleman, D.E., and Evans, H.T., Jr. (1973) Job 9214: Indexing and least-squares refinement of powder diffraction data. U.S. Geological Survey, Computer Contributions 20, 25 p.
- Eugster, H.P., and Wright, T.L. (1960) Synthetic hydrous boron micas. U.S. Geological Survey Professional Paper 400-B, 441–442.
- Foord, E.E., Starkey, H.C., and Taggart, J.E., Jr. (1986) Mineralogy and paragenesis of "pocket clays" and associated minerals in complex granitic pegmatites, San Diego County, California. *American Mineralogist*, 71, 428–439.
- Foord, E.E., Spaulding, L.B., Jr., Mason, R.A., and Martin, R.F. (1989) Mineralogy and paragenesis of the Little Three Mine pegmatites, Ramona district, San Diego County, California. *Mineralogical Record*, 20, 101–127.
- Frey, M., Hunziker, J.C., Jager, E., and Stern, W.B. (1983) Regional distribution of white K-mica polymorphs and their phengite content in the Central Alps. *Contributions to Mineralogy and Petrology*, 83, 185–197.
- Harder, H. (1959a) Beitrag zur Geochemie des Bors. I. Bor in Mineralen und magmatischen Gesteinen. Akademie der Wissenschaften in Göttingen, Mathematisch-physikalische Klasse, Nachrichten, 5, 67–122.
- (1959b) Beitrag zur Geochemie des Bors. II. Bor in Sedimenten. Akademie der Wissenschaften in Göttingen, Mathematisch-physikalische Klasse, Nachrichten, 6, 123–183.
- Hawthorne, F.C., and Černý, P. (1982) The mica group. In P. Černý, Ed., *Mineralogical Association of Canada Short Course Handbook*, 8, 63–98.
- Lacroix, A. (1922) *Minéralogie de Madagascar*, vol. 1. Editions Aug. Chailamel, Paris.
- Livi, K.J.T., and Veblen, D.R. (1987) "Eastonite" from Easton, Pennsylvania: A mixture of phlogopite and a new form of serpentine. *American Mineralogist*, 72, 113–125.
- London, D. (1984) Experimental phase equilibria in the system LiAlSiO<sub>4</sub>-SiO<sub>2</sub>-H<sub>2</sub>O: A petrogenetic grid for lithium-rich pegmatites. *American Mineralogist*, 69, 995–1004.
- (1986a) The magmatic-hydrothermal transition in the Tanco rare-element pegmatite, Manitoba: Evidence from fluid inclusions and phase equilibrium experiments. *American Mineralogist*, 71, 376–395.
- (1986b) Formation of tourmaline-rich gem pockets in miarolitic pegmatites. *American Mineralogist*, 71, 396–405.
- (1987) Internal differentiation of rare-element pegmatites: Effects of boron, phosphorus, and fluorine. *Geochimica et Cosmochimica Acta*, 51, 403–420.
- Mukhamet-Galeyev, A.P., Zotov, A.V., Pokrovskiy, V.A., and Kotova, Z.Yu. (1984) Stability of the 1M and 2M<sub>1</sub> polytypic modifications of muscovite as determined from solubility at 300° at saturation steam pressure. *Doklady Akademii Nauk SSSR*, 278, 2, 449–452 (in Russian).
- Noda, T., Daimon, N., and Toyoda, H. (1944) Synthesis of boron mica. *Journal of the Society of Chemical Industry of Japan*, 47, 499–502 (in Japanese).
- Ranorofoa, N., Fontan, F., and Fransolet, A.-M. (1989) Rediscovery of manandonite in the Sahatany Valley, Madagascar. *European Journal of Mineralogy*, 1, 633–638.
- Stern, L.A., Brown, G.E., Jr., Bird, D.K., Jahns, R.H., Foord, E.E., Shigley, J.E., and Spaulding, L.B., Jr. (1986) Mineralogy and geochemical evolution of the Little Three pegmatite-aplite layered intrusive, Ramona, California. *American Mineralogist*, 71, 406–427.
- Taylor, B.E., Foord, E.E., and Friedrichson, H. (1979) Stable isotope and fluid-inclusion studies of gem-bearing granitic pegmatite-aplite dikes, San Diego County, California. *Contributions to Mineralogy and Petrology*, 68, 187–205

MANUSCRIPT RECEIVED MARCH 19, 1990

MANUSCRIPT ACCEPTED JUNE 26, 1991